A NATURE INSPIRED GUIDANCE METHOD FOR IMPROVING SOCIAL ACCEPTANCE OF URBAN AIR MOBILITY

Zeynep Bilgin *
Technical University of Munich
Munich, Germany

Murat Bronz †
ENAC, Université de Toulouse
Toulouse, France

İlkay Yavrucuk ‡
Technical University of Munich
Munich, Germany

This work introduces a nature-inspired guidance method to enhance social acceptance of urban air mobility. A dynamic crowd avoidance feature is integrated to the guidance algorithm to improve safety, reduce noise, and enhance positive public perception. To further improve the safety of the system, an emergency landing mode is introduced. To perform landing maneuver and fully utilize the urban airspace, the guidance algorithm is extended from 2D to 3D while maintaining real-time capability and low computational load. Scaled hardware experiments are conducted to asses the effectiveness of the proposed guidance approach. Experiments demonstrate effective crowd avoidance and emergency landing while ensuring collision and obstacle avoidance. Proposed enhancements show potential to promote public acceptance of urban air mobility systems by improving safety while maintaining efficiency.

1 INTRODUCTION

As cities continue to grow, the need for efficient and sustainable transportation systems has become increasingly important. Expanding the urban transportation to urban airspace is a promising solution for urban mobility problem. However, implementation of this innovative mobility solution is not devoid of complexities. Development of a sustainable transportation policy and service can prove to be challenging as such a problem often has vague boundaries and involves multiple stakeholders with conflicting values [1]. This is also the case for urban air mobility where safe, sustainable and efficient deployment requires collaboration of people and organizations with different perspectives [2]. A significant challenge in employing air mobility as a means of urban transport is securing public acceptance, as community resistance is the most likely risk that could undermine the viability of the transport system [3]. To diminish this threat and ensure sufficient community engagement, it is essential to take public concerns and feedback into account when designing a transportation system. Survey conducted among European Union(EU)-Citizens indicate that the most common concerns of EU-Citizens about Urban Air Mobility (UAM) operations are safety, noise and visual impact and security [4–9]. Addressing these concerns is the key to public acceptance and can enable successful implementation of Urban Air Mobility concepts.

In this paper, a nature inspired guidance method, previously proposed in [10, 11] is further modified to improve social acceptance of Urban Air Mobility operations. The social aspects considered in this study are concerns for safety, noise and visual pollution.

Projected use cases of urban air mobility services in 2035-time horizon indicate low number of automatic personal aerial transportation [3]. Hence, when discussing safety concerns it is more appropriate

* PhD Candidate, zeynep.bilgin@tum.de
† Assistant Professor, murat.bronz@enac.fr
‡ Professor, ilkay.yavrucuk@tum.de

to consider entire population inhabiting the city [4] as opposed to only service users as majority of the population will not use aerial transportation services but will be affected by them. This study focuses on improving the safety of aerial transportation both for service users and other affected parties by integrating a crowd avoidance system to the guidance algorithm. Avoiding crowds not only improves the safety but also can reduce the exposure to noise and visual pollution; thus can have a positive impact on public acceptance. Although blocking certain regions in a city ensures avoiding crowds, this approach reduces the efficiency of the air mobility system as vehicles cannot use these routes even when streets are empty. Instead, more dynamic approach can guarantee the safety of citizens while maintaining the efficiency of the mobility system. This paper introduces an automatic crowd avoidance feature embedded into the guidance system. After location and the radius of the crowd is specified, the vehicles can automatically avoid this region and continue avoiding collision with each other and buildings at the same time.

An other safety enhancement feature considered in this work is addition of an emergency landing system to the guidance algorithm. The ability to perform an unscheduled landing in case of a failure is one of the safety requirements for urban air mobility vehicles [12]. The emergency can occur at any moment without any warning or priory knowledge. When it occurs, the defected vehicle is automatically guided to the nearest emergency landing pad while all the other vehicles in the vicinity move away from the defected vehicle to prevent any collision and ensure a safe landing. To better model the landing maneuver, existing 2D guidance algorithm is extended to 3D. By introducing 3D flow elements movement in vertical direction is induced. To maintain both obstacle avoidance capability and low computational load, instead of using 3D building models, 2D cross-sections stacked on top of each other is preferred.

Conducting experiments is an essential part of evaluating the performance of any guidance method. Effectiveness of proposed method is demonstrated both through scaled hardware experiments. The experiments are conducted in The Toulouse Occitanie Drone Flight Area located in France. The platform offers the possibility of conducting experiments with micro-drones and embedded systems in one of the most hi-tech instrument equipped indoor flight zones in Europe [13].

Contributions of this work is threefold. First, existing 2D guidance algorithm is extended to 3D while maintaining its low computational load property and real time solution capability. Secondly, crowd avoidance feature is integrated into the guidance algorithm. Vehicles are enabled to avoid crowded regions within the city while traveling to their destination. With this feature, safety of operations in urban airspace is aimed to be improved. Furthermore, population avoidance also reduces the visual pollution and noise and can enhance positive public perception to urban air mobility services. Last but not least, an emergency landing mode is included in the guidance algorithm to further improve the safety. In case of a failure, defected vehicle can be guided to the nearest emergency landing pad while other vehicles in the vicinity avoid the faulty vehicle.

2 VECTOR FIELD BASED GUIDANCE METHOD

In this study previously presented vector field based guidance algorithm is employed [10, 11, 14]. The guidance algorithm imitates fluid flow around obstacles and uses potential flow equations to generate a guidance vector field. Analytical solutions can be obtained for obstacles with simpler shapes such as circles and ellipses. To generate the flow field around arbitrarily shaped obstacles a numerical tool called panel method is utilized. In this approach, the obstacle boundary is divided into small line segments called panels and the vector filed around the obstacle generated by the fluid can be calculated by solving a system of linear equations in Equation 1.

$$K_{ij}\gamma_j = RHS_i \tag{1}$$

Here, K is a coefficient matrix and γ_j is the unknown vortex strength on panel j. Components of K_{ij} are the

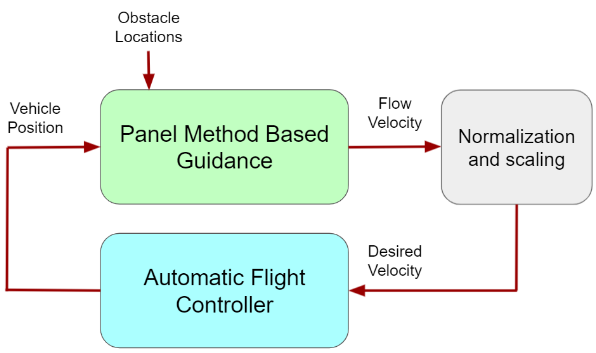

Fig. 1: Block diagram for proposed guidance method. Obstacle and vehicle positions are fed to the guidance algorithm as input and desired velocity vector that guarantees collision avoidance is generated.

normal velocity induced by jth panel on ith panel as given in Equation 2.

$$K_{ij}\gamma_j = (u,v)_{ij} \cdot \vec{n}_i \quad (2)$$

The RHS vector in Equation 1 contains the known flow components in the arena. Block diagram for proposed guidance method is presented in Figure 1.

Obstacle and vehicle positions are fed to the guidance algorithm as input. The flow velocity at a point of interest; that is, vehicle's current position, is calculated at each time-step and then fed into automatic flight control system as desired velocity.

2.1 APPLICATION TO URBAN AIR MOBILITY

Panel method based guidance algorithm can be modified to fit to the urban air mobility problem [10,14]. Following [15, 16] and [10, 14], an ideal fluid is contained in a region $\mathscr{D}$ in $\Re^2$. Let $P = (x,y)^T$ be any arbitrary point in $\mathscr{D}$. The velocity of the fluid at any point in $\mathscr{D}$ is denoted by $V = (u,v)^T$. By potential flow theory, the flow velocity at any point $P = (x,y)^T \in \mathscr{D}$ can be calculated using Equation 3 and Equation 4.

$$u = \frac{-\sigma_g}{2\pi}\frac{x-x_g}{r_g^2} + \sum_{s=1}^{S}\sum_{k=1}^{K}\frac{\gamma_{sk}}{2\pi}\frac{x-x_{sk}}{r_{sk}^2} + u_\infty \quad (3)$$

$$v = \frac{-\sigma_g}{2\pi}\frac{y-y_g}{r_g^2} + \sum_{s=1}^{S}\sum_{k=1}^{K}\frac{-\gamma_{sk}}{2\pi}\frac{y-y_{sk}}{r_{sk}^2} + v_\infty \quad (4)$$

Here, u_∞ and v_∞ are components of the free stream velocity. S and K are number of obstacles(buildings) and number of panels on obstacle boundaries respectively. Position of a vortex element on a given obstacle and panel is denoted as (x_{sk}, y_{sk}) and associated vortex strength is γ_{sk}. The goal position is denoted by $P_g = (x_g, y_g)^T$ and modelled by a point sink element with strength σ_g.
Furthermore, in order to prevent collisions between vehicles in real time, each vehicle is modelled as a point source element and the flow velocities are recalculated as in Equation 5 and Equation 6

$$u = \frac{-\sigma_g}{2\pi}\frac{x-x_g}{r_g^2} + \sum_{n=1}^{N}\frac{\sigma_n}{2\pi}\frac{x-x_n}{r_n^2} + \sum_{s=1}^{S}\sum_{k=1}^{K}\frac{\gamma_{sk}}{2\pi}\frac{x-x_{sk}}{r_{sk}^2} \quad (5)$$

$$v = \frac{-\sigma_g}{2\pi}\frac{y-y_g}{r_g^2} + \sum_{n=1}^{N}\frac{\sigma_n}{2\pi}\frac{y-y_n}{r_n^2} + \sum_{s=1}^{S}\sum_{k=1}^{K}\frac{-\gamma_{sk}}{2\pi}\frac{y-y_{sk}}{r_{sk}^2} \quad (6)$$

Here, N is the total number of vehicles in the airspace and σ_n is the source strength of each vehicle to prevent collisions. Position of vehicles are denoted as $P_n = (x_n, y_n)^T$.
Additionally, respecting current air traffic control regulations, an additional vortex element is assigned to each vehicle. This vortex element forces vehicles to always alter their course to the right in case of a conflict imposing the so called "Right of way" rule in tactical conflict resolution.

$$\begin{aligned} u = &\frac{-\sigma_g}{2\pi}\frac{x-x_g}{r_g^2} + \sum_{n=1}^{N}\frac{\sigma_n}{2\pi}\frac{x-x_n}{r_n^2} + \frac{\gamma_n}{2\pi}\frac{x-x_n}{r_n^2} \\ &+ \sum_{s=1}^{S}\sum_{k=1}^{K}\frac{\gamma_{sk}}{2\pi}\frac{x-x_{sk}}{r_{sk}^2} \end{aligned} \quad (7)$$

$$\begin{aligned} v = &\frac{-\sigma_g}{2\pi}\frac{y-y_g}{r_g^2} + \sum_{n=1}^{N}\frac{\sigma_n}{2\pi}\frac{y-y_n}{r_n^2} + \frac{-\gamma_n}{2\pi}\frac{y-y_n}{r_n^2} \\ &+ \sum_{s=1}^{S}\sum_{k=1}^{K}\frac{-\gamma_{sk}}{2\pi}\frac{y-y_{sk}}{r_{sk}^2} \end{aligned} \quad (8)$$

The vortex element is included into calculations as given in Equation 7 and Equation 8.
Panel method requires vehicle positions and obstacle position as input. First, Equation 1 has to be solved for unknown vortex strengths. Coefficient matrix K in Equation 1 is a constant and can be calculated and inverted offline to reduce computational load. After vortex strengths are found, flow velocity at current vehicle position can be calculated using Equation 3 and Equation 4.
Reader may refer to [10,11,17] for detailed derivation of method.

2.2 GUIDANCE IN 3-D

In this paper, existing 2 dimensional guidance method is further extended to 3rd dimension. Although it is possible to implement model obstacles in 3D and solve for 3D flow field around the obstacles, introducing the 3rd dimension to the obstacle model would increase the number of panels required for solution and in turn the overall computational load immensely. Instead, an alternative approach is considered in order to maintain the real-time solution capability of the guidance method. In this approach, only the 2-D cross-section of buildings at relevant altitude are considered and modelled as 2-D obstacles. Destinations and vehicles, on the other hand, are modelled as 3-D point sinks and sources respectively.

$$u = \frac{-\sigma_g}{2\pi}\frac{x-x_g}{r_g^2} + \sum_{n=1}^{N}\frac{\sigma_n}{2\pi}\frac{x-x_n}{r_n^2} + \sum_{s=1}^{S}\sum_{k=1}^{K}\frac{\gamma_{sk}}{2\pi}\frac{x-x_{sk}}{r_{sk}^2} \quad (9)$$

$$v = \frac{-\sigma_g}{2\pi}\frac{y-y_g}{r_g^2} + \sum_{n=1}^{N}\frac{\sigma_n}{2\pi}\frac{y-y_n}{r_n^2} + \sum_{s=1}^{S}\sum_{k=1}^{K}\frac{-\gamma_{sk}}{2\pi}\frac{y-y_{sk}}{r_{sk}^2} \quad (10)$$

$$w = \frac{-\sigma_g}{4\pi}\frac{z-z_g}{r_g^3} + \sum_{n=1}^{N}\frac{\sigma_n}{4\pi}\frac{z-z_n}{r_n^3} \quad (11)$$

Hence, the motion of the vehicle in plane is governed by combined effect of 2-D obstacles and relevant components of the sources and sinks as given in Equation 9 and Equation 10. Vehicle altitude is controlled solely by the effect of 3-D source and sink elements as given in Equation 11. As vehicles change altitude, building cross-sections can also be updated to ensure collision free flight. This approach, enables vehicles to change altitude throughout the flight, ascend or descend towards their goal positions without risk of collision with obstacles or other vehicles in the same airspace while also maintaining low computational cost of panel method solution.

2.3 MODELING POPULATION

One way to improve the safety of service users and population inhabiting the city is for vehicles to avoid flying across crowded regions. Although defining certain regions as no-fly zones at all times ensures avoiding crowds, it reduces the efficiency of the air mobility system by preventing vehicles to take shorter routes when streets are empty. In this case, more dynamic approach can ensure safety of citizens without jeopardizing mobility system's efficiency. To achieve that, populations throughout the city are modeled as point sources with variable strength. Populations can pop-up dynamically and their strength can grow as the region gets more crowded or vanish if the crowd dissipates. The source element can also move if population also travels within the city. The flow velocity ensuring crowd and collision avoidance in the city can be calculated using Equation 12 ,Equation 13 and Equation 14.

$$\begin{aligned} u = &\frac{-\sigma}{2\pi}\frac{x-x_g}{r_g^2} + \sum_{n=1}^{N}\frac{\sigma_n}{2\pi}\frac{x-x_n}{r_n^2} \\ &+ \sum_{m=1}^{M}\frac{\sigma_m}{2\pi}\frac{x-x_m}{r_m^2} + \sum_{s=1}^{S}\sum_{k=1}^{K}\frac{\gamma_{sk}}{2\pi}\frac{x-x_{sk}}{r_{sk}^2} \end{aligned} \quad (12)$$

$$\begin{aligned} v = &\frac{-\sigma}{2\pi}\frac{y-y_g}{r_g^2} + \sum_{n=1}^{N}\frac{\sigma_n}{2\pi}\frac{y-y_n}{r_n^2} \\ &+ \sum_{m=1}^{M}\frac{\sigma_m}{2\pi}\frac{y-y_m}{r_m^2} + \sum_{s=1}^{S}\sum_{k=1}^{K}\frac{-\gamma_{sk}}{2\pi}\frac{y-y_{sk}}{r_{sk}^2} \end{aligned} \quad (13)$$

$$w = \frac{-\sigma_g}{4\pi}\frac{z-z_g}{r_g^3} + \sum_{n=1}^{N}\frac{\sigma_n}{4\pi}\frac{z-z_n}{r_n^3} + \sum_{m=1}^{M}\frac{\sigma_m}{4\pi}\frac{z-z_m}{r_m^3} \quad (14)$$

Here, (x_g, y_g) and σ are goal position and sink strength associated with this goal position respectively. N is the total number of vehicles in the arena and each vehicle has a source assigned to them with strength σ_n. M is the total number of restricted zones in the arena and each zone has a source assigned to them with strength σ_m. S and K are number of obstacles and number of panels respectively.

3 EXPERIMENT SETUP

Experiments for this study are conducted in the indoor test facility, The Toulouse Occitanie Drone Flight Arena, located in Toulouse, France. A scaled urban environment is built in the $8\text{m}\times 8\text{m}\times 8\text{m}$ flight area as shown in Figure 2a. Test environment is equipped with high-precision localisation and measuring instruments that include an Opti-Track system with 16 cameras that can work at 320Hz. The camera system can also locate the position of the buildings and position of the population which is represented by the red ball placed at the lower right corridor in the scaled city in Figure 2a. It is possible to use different types of vehicles in the experiments. For this study an off the shelf quad-rotor shown in Figure 2b is considered. Tello EDU quad-rotors are equipped with 2.4 GHz 802.11n Wi-Fi and are controlled through a ground station. The quad-rotors have a built in automatic flight controller that directly accepts translation velocity and internally tries to follow the given reference velocity by comparing to its on-board velocity estimation coming from downward looking optic-flow camera.

4 RESULTS AND DISCUSSION

Conducting experiments is an essential part of validation of any guidance method. In this study, indoor flight tests are conducted to asses the effectiveness of proposed modifications to the guidance method. All flight tests are conducted in the same urban configuration with the same mission to better compare the effects of modifications in the guidance algorithm.

(a) The Toulouse Occitanie Drone Flight Arena

(b) Tello EDU Quad-rotor

Fig. 2: Experimental Setup. Flight tests are conducted in the indoor flight arena located in Toulouse, France. For the experiments an off the shelf Tello EDU quad-rotor is used.

In Figure 3 flight arena setup and vertiport locations are shown together with vertiport visiting order for each individual vehicle. Magenta shapes are the 2-D cross-section of buildings in the scaled urban arena. Although panel method solution can generate flow field around any arbitrarily shaped object, square and hexagon obstacles are selected for ease of manufacturing. Each building is expanded by the amount of vehicle radius to ensure safety. Expanded safety regions are plotted in lighter color around each building. Four vertiports are placed in between five buildings as shown in Figure 3a. Throughout the flight test campaign each vehicle follows a specific task assigned to themselves. Vehicle tasks are visualized in Figure 3b. Each vehicle has its pre-specified starting position and vertiport visiting order. Once a vehicle visits all vertiports, it returns to its starting position and starts over the task until the test is stopped. The blue vehicle starts from 'V4' and travels in clockwise direction between consecutive vertiports. Similarly, the red vehicle starts from 'V1' and travels in counter clockwise direction. Finally, the green vehicle travels in the order: V2-V4-V1-V3-V2 as shown in Figure 3b. These tasks are designed to better demonstrate collision avoidance capability of the proposed guidance method as vehicles traveling in opposite direction in the same route are bound to encounter and are forced to perform an avoidance maneuver.

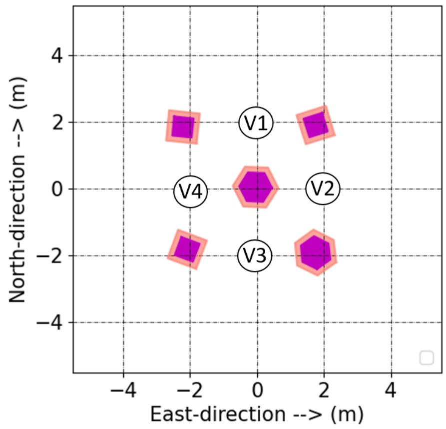

(a) Flight arena setup and vertiport locations.

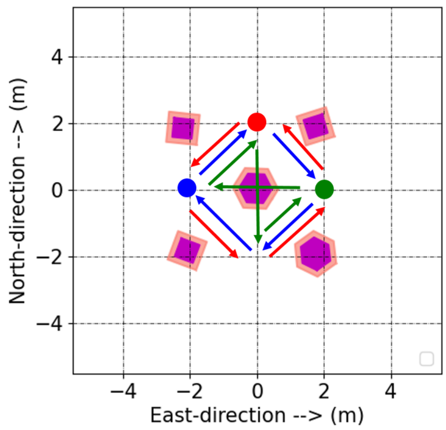

(b) Vertiport visit order for each individual vehicle.

Fig. 3: Flight arena setup and vehicle tasks. Four vertiports are located between five buildings. Vehicles are tasked with flying between vertiports in the order indicated by arrows.

4.1 NOMINAL CASE

In Figure 4 flight test results for the nominal case can be seen. In this scenario, vehicles are to rotate between vertiports in specified order until the test is over. All vehicles travel between their destinations while avoiding collision with each other and the buildings around them at the same time. The trajectories to be followed are not provided to the

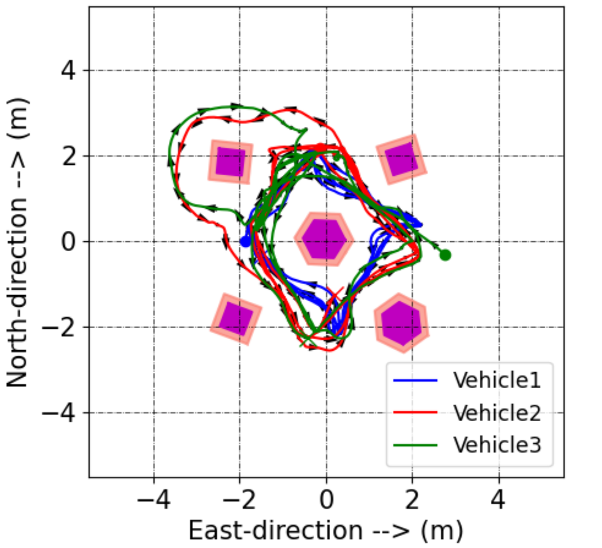

(a) Flight test results for nominal case in 2D view.

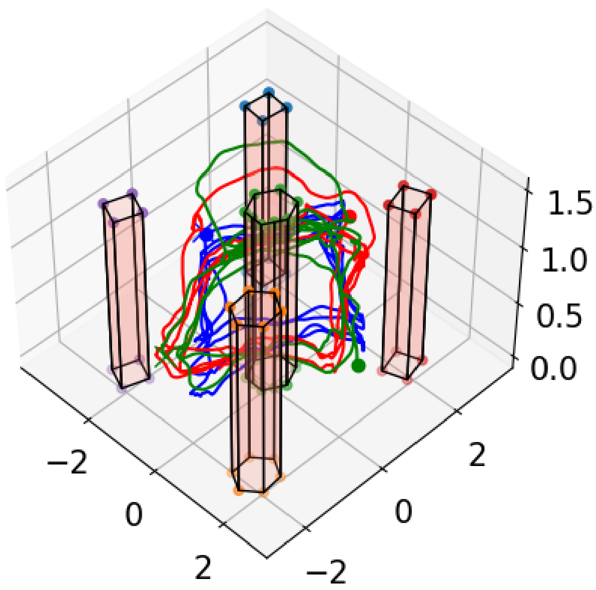

(b) Flight test results for nominal case in 3D view.

Fig. 4: Flight test results for nominal case plotted in 2D and 3D views. Each vehicle follows a specific order to visit all vertiports while avoiding collision with other vehicles and buildings

vehicles, instead at each time-step vehicles calculate a desired velocity vector that leads them to their goal while guaranteeing collision avoidance. Notice that, when a corridor between buildings gets too crowded vehicles choose to take a detour around buildings to avoid collision with each other.

Flow velocity is faster near sources and sinks. Following such a velocity profile is not desirable for urban air mobility applications due to safety concerns. Accelerating when approaching to a vertiport or to other vehicles increases collision risk. To achieve a more desirable velocity profile, sink strength assigned to goal positions are adjusted such that when the vehicle is away from the sink the sink strength grows and as the vehicle approaches to its destination sink strength is reduced. This way vehicle can travel at higher speeds towards its goal and slow down as it approaches to the final destination. Similarly, source strengths assigned to other vehicles are also adjusted with respect to the changing sink strength. This way, instead of suddenly accelerating to avoid each other, vehicles slow down, come to a stop and then change direction if necessary. Velocity profiles for each vehicle in nominal case are given in Figure 5.

4.2 POPULATION AVOIDANCE

In this scenario, a population increase is introduced in the city. Flying over crowded regions jeopardizes the safety of the population on the ground in case of a catastrophic failure. Furthermore, even without a failure, such flights disturb peace due to noise and visual pollution generated by urban air mobility vehicles. Hence, avoiding crowds is not only safer but also can promote social acceptance. In this scenario, when a certain region in the city gets crowded, vehicle are notified and avoid flying over this section of the city. Vehicles are ordered to follow the exact same sequence between vertiports as in the nominal case. Flight tests results are presented in Figure 6. The densely populated area is marked with an orange circle. Notice the difference between the resultant trajectories followed by vehicles compared to those presented in Figure 4 for the nominal case. In this scenario, vehicles not only avoid the crowded street but also avoid collision with buildings and each other.

4.3 EMERGENCY LANDING

The final scenario considered in this study is performing an emergency landing in case of a failure. This work considers a failure such that the failed vehicle is not able to continue its mission but is able to maneuver and land to the nearest emergency landing pad. Emergency landing pads are located near vertiports as shown in Figure 7. Other vehicles in the airspace can continue their missions normally and avoid the failed vehicle to prevent any accidents. For fight tests, no real failure is induced on the vehicles. Instead, during the mission selected vehicle is informed that it is experiencing a failure and should immediately perform an emergency landing on the nearest emergency landing pad. Vehicles do not have

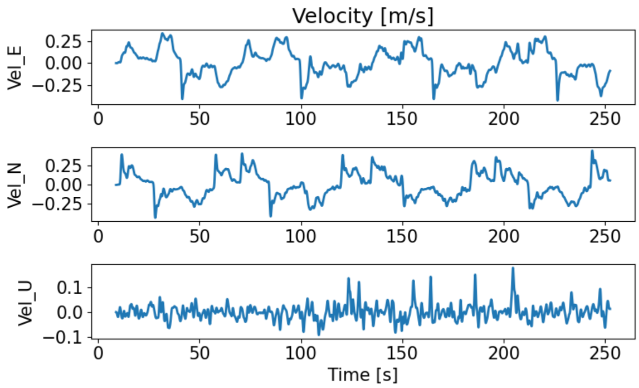

(a) Velocity change for Vehicle 1.

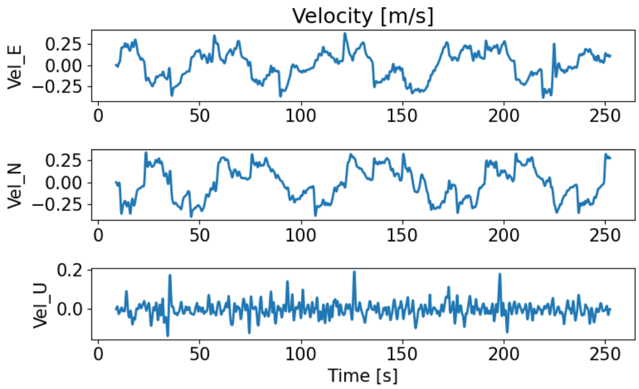

(b) Velocity change for Vehicle 2.

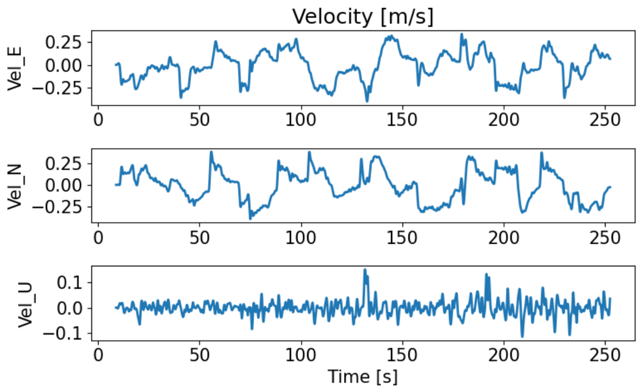

(c) Velocity change for Vehicle 3.

Fig. 5: Velocity change for vehicles with respect to time in nominal case. Vehicles slow down when approaching vertiports and when they encounter another vehicle.

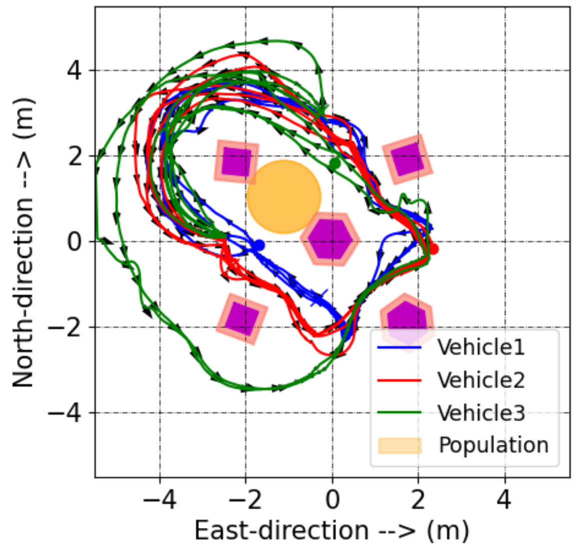

(a) Flight test results for nominal case in 2D view.

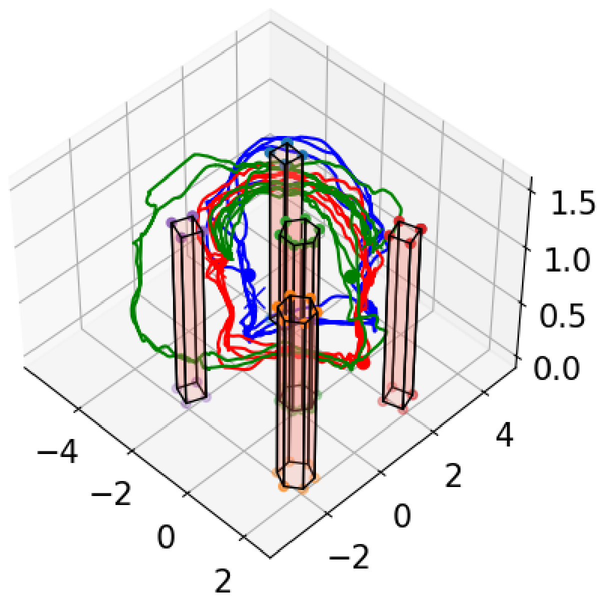

(b) Flight test results for nominal case in 3D view.

Fig. 6: Flight test results for the population avoidance case plotted in 2D and 3D view. Each vehicle follows its specific order to visit all vertiports while avoiding collision with other vehicles and buildings. Furthermore, vehicles also avoid the densely populated area in the city marked with orange circle.

priory knowledge on neither which vehicle will fail nor when will the failure occur. When the failure occurs, vehicles have to automatically alter their path and either perform the emergency landing or avoid the failed vehicle and carry on with their mission.

Flight test results for emergency landing scenario are plotted in Figure 8. Here, 40 seconds after the start of their missions, the blue vehicle is notified that it is experiencing a failure and should land. The selected vehicle abandons its mission and locates the nearest emergency landing pad to perform an emergency landing. Red and green vehicles avoid the blue vehicle and carry on with their respective missions. In Figure 9 flight test results for the emergency landing scenario is plotted in 3D view together with altitude changes of vehicles with respect to time. For this scenario, each vertiport is placed at a different altitude and the emergency landing pad is located

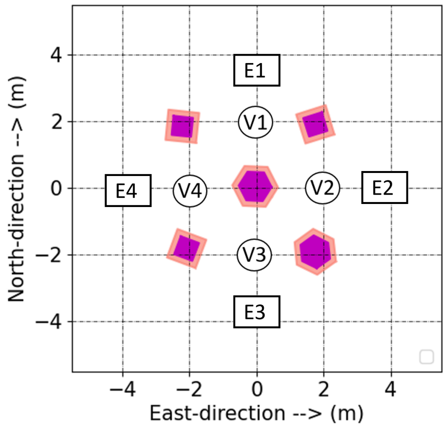

Fig. 7: Flight arena setup with vertiport locations and emergency landing pads. There are four emergency landing pads located near vertiports.

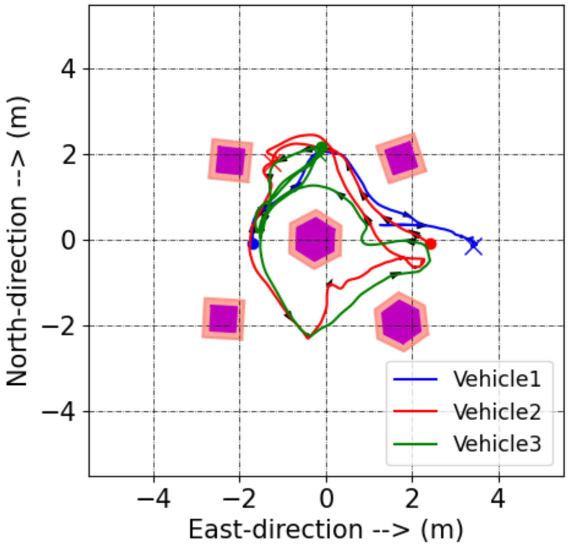

Fig. 8: Flight test results for the emergency landing case. Blue vehicle experiences a failure without prior knowledge, locates the nearest emergency landing pad and performs a landing. Red and green vehicles avoid the blue vehicle and continue with their missions.

at 0.4 meters which is the reference zero that can be detected by the Opti-Track system. In Figure 9b altitude change of vehicles with respect to time is plotted. Oscillations in the altitude are originated from the altitude hold feature of the on-board automatic flight controller. Notice that, at $t = 40.0$ seconds, the blue vehicle not only changes its heading towards the emergency landing pad but also starts its descend.

5 CONCLUSIONS

This paper addresses the public acceptance concerns associated with implementing urban air mobility as a transportation solution. The primary goal of this study

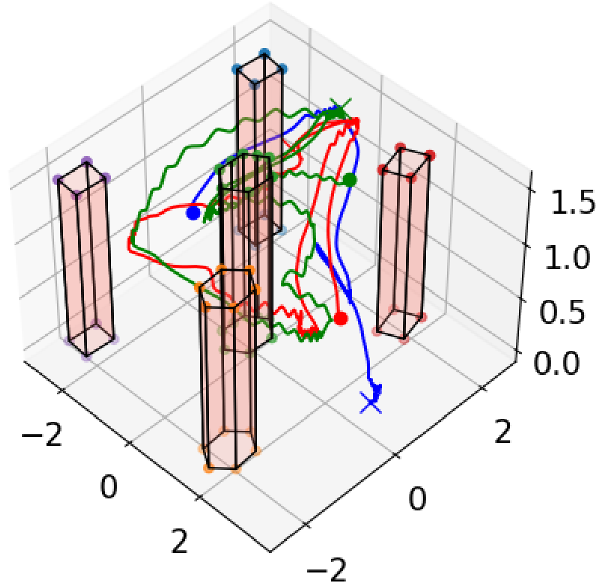

(a) Flight test results for the emergency landing case in 3D view.

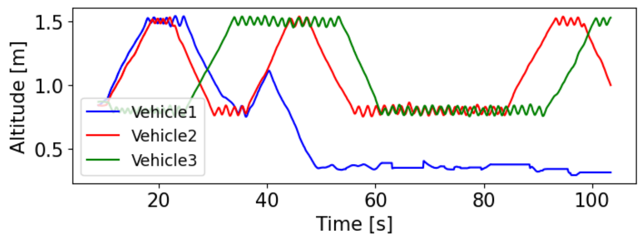

(b) Altitude change of vehicles for the emergency landing case.

Fig. 9: Flight test results for the emergency landing case in 3D view and altitude changes. Each vertiport is located at a different altitude modelled by a 3D sink element making vehicles to climb or descent between destinations. Emergency landing pad is also a 3D sink element enables vehicle to perform an automatic landing maneuver.

is to enhance the social acceptance and safety of urban air mobility operations through the integration of crowd avoidance and emergency landing features into a vector field-based guidance algorithm.

Through hardware experiments in an indoor flight arena, the proposed modifications to the guidance algorithm are tested. The experiment results demonstrates the effectiveness of the proposed guidance approach in achieving dynamic crowd avoidance while maintaining collision and obstacle avoidance. Furthermore, an emergency landing feature is also introduced to address safety concerns in the event of an unforeseen failure. During flight tests, the guidance algorithm successfully guided a failed vehicle to the nearest emergency landing pad, while allowing other vehicles to continue their missions uninterrupted. Finally, to guide the vehicles throughout the landing maneuver, 2D guidance algorithm is extended to 3D. Instead of including 3D building models to the calculations, 2D cross-sections of buildings are stacked to maintain low computational load and real-time guidance capability.

Several challenges are encountered during the course of this work. Firstly, the oscillations in altitude hold caused by the quad-rotors' on-board automatic flight controller require further attention to achieve smoother flight trajectories. Secondly, while the stacking of 2D cross-sections of buildings provides obstacle avoidance at low computational cost, it poses limitations for maneuvers such as ascending and navigating over buildings. Finally, the source strength assigned to the population is a design parameter to be fine-tuned. Finding the balance between pushing vehicles sufficiently away from crowded areas and preventing excessive avoidance remains a challenge. Moreover, the potential for stagnation points arising from the combined effect of sources and sinks demands further investigation, particularly when the population is situated close to the goal positions.

To summarize, contributions of this study are extending the existing 2D guidance algorithm to 3D, integrating crowd avoidance feature, and incorporating an emergency landing mode to the guidance algorithm. These enhancements collectively promote safer and more socially acceptable urban air mobility operations. Experimental results indicate the proposed guidance algorithm can be an effective tool for the successful implementation of urban air mobility systems in the future.

ACKNOWLEDGMENT

This work has been partially funded by the ENAC Drones and UTM Research Chair via ENAC Foundation sponsors Airbus and SopraSteria.

6 REFERENCES

[1]Mitchell, V., Ross, T., May, A., Sims, R., and Parker, C., "Empirical investigation of the impact of using co-design methods when generating proposals for sustainable travel solutions," *CoDesign*, Vol. 12, No. 4, 2016, pp. 205–220.

[2]Bardwell, P. and Marr, S., "Making the Most of Collaboration: An International Survey of Public Service Co-Design, DEMOS Report 23," Tech. rep., DEMOS, Price Waterhouse Coopers (PWC) Public Sector Research Centre, London, 2008.

[3]ASSURED-UAM, "Financing and public acceptance," H2020-EU.3.4. - SOCIETAL CHALLENGES - Smart, Green And Integrated Transport, DOI: 10.3030/101006696, 2021.

[4]EASA, "Study on the societal acceptance of Urban Air Mobility in Europe," *European Union Aviation Safety Agency*, 2021.

[5]CAMI, "Components of Public Acceptance for AAM and UAM," *The Community Air Mobility Initiative*, 2020.

[6]Boucher, P., "'You Wouldn't have Your Granny Using Them': Drawing Boundaries Between Acceptable and Unacceptable Applications of Civil Drones," *Sci Eng Ethics*, Vol. 22, 2016.

[7]Finn, R. L., Wright, D., Jacques, L., and Hert, P. D., "Study on privacy, data protection and ethical risks in civil Remotely Piloted Aircraft Systems operations," *European Commission*, 2014.

[8]Eissfeldt, H., Vogelpohl, V., Stolz, M., Papenfuss, A., Biella, M., Belz, J., and Kügler, D., "The acceptance of civil drones in Germany," *CEAS Aeronautical Journal*, 2020.

[9]TindAIR, "Social acceptance assesment report." H2020-SESAR-2020-1 SOCIETAL CHALLENGES - Smart, Green And Integrated Transport, DOI: 10.3030/101017677, 2022.

[10]Bilgin, Z., Bronz, M., and Yavrucuk, I., "Experimental Evaluation of Panel-Method-Based Path Planning for eVTOL in A Scaled Urban Environment," *Vertical Flight Society Forum 78*, May 10-12 2022.

[11]Bilgin, Z., Bronz, M., and Yavrucuk, I., "Experimental Evaluation of Robustness of Panel-Method-Based Path Planning for Urban Air Mobility," *AIAA Aviation Forum*, 27 June-1 July 2022.

[12]"European Union Aviation Safety Agency, Proposed Means of Compliance with the Special Condition VTOL (MOC SC-VTOL) 25 May 2020," May 25 2020.

[13]ENAC, "Drone Flight Arena Toulouse Occitanie," Ecole Nationale de l'Aviation Civile, Retrieved 19 October 2021, from `https://www.enac.fr/en/drone-flight-arena-toulouse-occitanie-0`.

[14]Bilgin, Z., Bronz, M., and Yavrucuk, I., “Panel Method Based Guidance for Fixed Wing Micro Aerial Vehicles,” *International Micro Air Vehicle Conference and Competition*, Sep 2022.

[15]Anderson, J. D., *Fundamentals of Aerodynamics*, McGraw-Hill, 5th ed., 2011.

[16]Katz, J. and Plotkin, A., *Low Speed Aerodynamics*, Cambridge Univ. Press, Cambridge, UK, 2001.

[17]Unal, Z. and Yavrucuk, I., “Panel Method Based Path Planning for eVTOL in Urban Environment,” *Vertical Flight Society Forum 77*, May 10-14 2021.